# Experimental Landau-Zener Tunneling (LZT) for Wave Redirection in Nonlinear Waveguides

Chongan Wang,[1,*] Ali Kanj,[1,*] Alireza Mojahed,[1] Sameh Tawfick,[1,2,†] and Alexander F. Vakakis[1,†]

[1] *Department of Mechanical Science and Engineering, University of Illinois at Urbana-Champaign, United States of America*

[2] *The Beckman Institute for Advanced Science and Technology, University of Illinois at Urbana-Champaign, United States of America*

(Dated: August 27, 2020)

We present an acoustic analog of the Landau-Zener Tunneling (LZT) quantum mechanical effect and apply it for irreversible wave redirection in weakly coupled nonlinear waveguides under impulse excitation. Due to nonlinearity, LZT-induced wave redirection is passively self-tunable with energy, being realized only in a certain energy band, that can be precisely predicted by theoretical models. Apart from the macroscale experimental validation of the classical quantum LZT effect, the findings apply to a broad class of acoustical systems with nonlinearity, disorder, and weak coupling.

Keywords: Landau-Zener Tunneling; acoustic waves; passive wave redirection; self-tunable waveguides

## I. INTRODUCTION

Landau-Zener Tunneling (LZT) denotes non-adiabatic energy tunneling in a quantum mechanical system, across an energy gap between two anti-crossed energy levels [1, 2]. LZT has been observed in various fields, including semiconductor superlattices [3, 4], optical fields [5, 6], Bose-Einstein condensates [7, 8], ultrasonic superlattices [9], phononic crystals [10, 11] and surface elastic waves [12]. The common feature in these applications is the intriguing irreversible resonance-induced energy transition between two states under external stimulation or perturbation. Perhaps the simplest analog of quantum LZT in classical mechanics is in two weakly coupled, identical pendulums; when one of the pendulum lengths slowly varies there occurs irreversible energy transfer between the pendulums due to parametric resonance [13, 14].

Here we provide experimental validation of a macroscale LZT analog in space for a system of two weakly coupled and disordered nonlinear waveguides under impulsive excitation. Recently, it was theoretically shown [15, 16] that LZT can yield to wave redirection in this system. Specifically, a symmetry-breaking variation of the spatial stiffness distribution in one of the waveguides induces LZT in space, resulting in irreversible breather redirection from the directly excited waveguide to the other. A break of symmetry was necessary for LZT, as in its absence wave localization [17–19] or recurrent wave exchanges [17–20] were realized. Analysis reduced the nonlinear acoustics of the coupled waveguides to a model of coupled oscillators with time-varying stiffness, enabling crossing eigenfrequencies in the time and resonance capture [16]. Moreover, due to nonlinearity the LZT-based wave redirection proved to be self-tunable to the intensity of the impulse and was realized only within a certain energy band; otherwise wave localization occurred [16].

Apart from the experimental demonstration of a macroscale analog in space of LZT, we confirm the efficacy of passive wave redirection in a system of impulsively excited acoustic waveguides with nonlinearity, weak coupling and spatial disorder. In addition, we highlight the self-tunability of LZT-based wave redirection to input energy, rendering the acoustical system passively self-adaptive to the external stimulant. Our experiments corroborate previous theoretical predictions and enable tunable-with-energy acoustic systems with inherent capacity for wave redirection.

## II. LZT IN THE REDUCED-ORDER MODEL (ROM)

The ROM of FIG. 1(a) consists of two waveguides, each with $n = 7$ unit-cells. We refer to the waveguide whose first unit-cell is subjected to an ideal impulse as "excited waveguide" – with unit-cells **E1**-**E7**, and to the other as "absorbing waveguide" – with unit-cells **A1**-**A7**. Each unit-cell is composed of a linearly grounded oscillator, coupled by essentially (i.e., non-linearizable) nonlinear springs to its adjacent unit-cells in the same waveguide, and by weak linear springs to the corresponding unit-cell in the other waveguide. The equations of motion are,

$$m\ddot{x}_1 + c_{g1}\dot{x}_1 + k_{g1}x_1 + k_e(x_1 - y_1) + c_e(\dot{x}_1 - \dot{y}_1) + c_{nl}(\dot{x}_1 - \dot{x}_2) + k_{nl}|x_1 - x_2|^{\beta-1}(x_1 - x_2) = F(t)\ , \qquad (1a)$$

[*] Contributed equally to this work

[†] Corresponding authors

$$m\ddot{x}_i + c_{g2}\dot{x}_i + k_{g2}x_i + k_e(x_i - y_i) + c_e(\dot{x}_i - \dot{y}_i) + c_{nl}(\dot{x}_i - \dot{x}_{i-1}) + c_{nl}(\dot{x}_i - \dot{x}_{i+1})$$
$$+k_{nl}|x_i - x_{i-1}|^{\beta-1}(x_i - x_{i-1}) \ + k_{nl}|x_i - x_{i+1}|^{\beta-1}(x_i - x_{i+1}) = 0 \ , \qquad 2 \leqslant i \leqslant n = 7, \tag{1b}$$

$$m\ddot{y}_i + c_{g1}\dot{y}_i + k_{g1}y_i + k_e(y_i - x_i) + c_e(\dot{y}_i - \dot{x}_i) + c_{nl}(\dot{y}_i - \dot{y}_{i-1}) + c_{nl}(\dot{y}_i - \dot{y}_{i+1})$$
$$+k_{nl}|y_i - y_{i-1}|^{\beta-1}(y_i - y_{i-1}) \ + k_{nl}|y_i - y_{i+1}|^{\beta-1}(y_i - y_{i+1}) = 0 \ , \qquad 1 \leqslant i \leqslant n = 7, \tag{1c}$$

with $y_0 \overset{\text{def}}{=} y_1$, $x_8 \overset{\text{def}}{=} x_7$, and $y_8 \overset{\text{def}}{=} y_7$, which denote the free boundary conditions of the boundary cells **A1**, **E7** and **A7**; the boundary cell **E1** is the one that is excited by the impulse $F(t) = I\delta(t)$, where $\delta(t)$ is Dirac's function and $I$ is the intensity of the impulse. Moreover, assuming zero initial conditions the applied impulse is equivalent to the initial condition $\dot{x}_1(0+) = I/m$ for unit-cell **E1**. In (1), $m$ denotes mass, and $k_{g1}$ and $k_{g2}$ the stiffnesses of the softer and stiffer linear groundings, respectively. The first unit-cell of the excited waveguide, and all unit-cells of the absorbing one possess softer grounding stiffnesses, $k_{g1} < k_{g2}$, breaking the symmetry. Also, $c_{g1}$ and $c_{g2}$ are the viscous damping coefficients of the soft and stiff groundings, respectively, whereas damping in the linear couplers is neglected, $c_e \sim 0$ [21]. Lastly, $k_{nl}$, $\beta$, and $c_{nl}$ are the stiffness coefficient, exponent, and linear damping coefficient of the nonlinear intra-waveguide coupling, respectively, and $k_e$ the stiffness of the linear inter-waveguide coupling. These were estimated by experimental system identification [21] and are given in TABLE I. Listed values and respective bracketed values (where applicable) are the mean and standard deviations of the identified parameters, respectively; otherwise, listed values are typical identified parameters.

For no spatial disorder, there are recurrent propagating breather exchanges [22] in the two waveguides, in a nonlinear beat phenomenon. With spatial disorder added, this evolves to irreversible breather redirection from the excited to the absorbing waveguide due to LZT [16]. This is shown by assuming a regime of irreversible breather redirection and introducing the variables:

$$u = \sum_{i=1}^{7} x_i \ ; \qquad v = \sum_{i=1}^{7} y_i \ . \tag{2}$$

Omitting damping, summing equations (1), and applying (2), the following linear system is obtained,

$$m\ddot{u} + k_{gE}(t)u + k_e(u - v) = 0 \ , \tag{3a}$$

$$m\ddot{v} + k_{g1}v + k_e(v - u) = 0 \ , \tag{3b}$$

where $u$ and $v$ denote the excited and absorbing "effective oscillators," respectively. The symmetry-breaking time-varying stiffness $k_{gE}(t)$ in (3a) reflects the change in the effective grounding stiffness as the breather propagates within the excited waveguide [15, 16], and converts the spatial disorder in (1) and temporal disorder in (3). Note that, initially the grounding stiffness of the excited effective oscillator is equal to the uniform grounding stiffnesses of the unit cells of the absorbing waveguide, $k_{gE}(t) \to k_{g1}$, whereas it subsequently increases to the value $k_{gE}(t) \to k_{g2}$ with increasing time. Therefore, the coupled effective oscillators (3a) and (3b) have two distinct time-dependent eigenstates; these eigenstates enable an initial 1:1 resonance capture between the two effective oscillators, and a subsequent escape from resonance capture as time progresses. The time scales governing the resonance capture and escape are governed by the weak coupling $k_e \ll \min\{k_{g1}, k_{g2}\}$ and the strong spatial stiffness disorder $k_e \ll |k_{g2} - k_{g1}|$. Based on these observations a three-stage model was created in [16] to analytically approximate the evolution of $k_{gE}(t)$; in that model $k_{gE}(t)$ equals $k_{g1}$ at the first stage, it linearly increases to $k_{g2}$ at the second stage, and then remains equal to $k_{g2}$ at the third stage. It is the second (non-adiabatic) stage that governs the irreversible energy transfer between the excited and absorbing effective oscillators. Indeed, due to the assumed weak coupling the dynamics of the effective system (3a) and (3b) exhibits fast-slow time scale separation in its transient dynamics [16], with the slow dynamics at the (critical) second stage being governed by Weber's equation, and yielding LZT and irreversible energy transfer. In turn, this analysis proves LZT wave redirection in the original nonlinear waveguides (1) for weak inter-waveguide coupling, strong stiffness disorder, and weak viscous dissipation. From TABLE I, our system parameters satisfy these requirements.

Note that LZT-based wave redirection is also realized when the nonlinear intra-waveguide coupling springs are replaced by linear ones (after all, LZT is a linear quantum effect). However, the nonlinearity enables self-tunability of wave redirection to input energy. To show this tunability, the mean (or typical) listed parameters of TABLE I are used to simulate the ROM (1) for varying initial velocities $\dot{x}_1(0+)$ of **E1**. The contour plot of FIG. 1(c) depicts energy penetration in the two waveguides, i.e., the maximum normalized energy of each unit-cell of the waveguides for the entire simulation. There are three different regimes for the acoustics distinguished by the intensity of the impulse. In the low energy (LE) regime (for initial velocities $\dot{x}_1(0+) < \sim 0.1$ m/s, the input energy is mainly localized in **E1** and **A1**. In the LE regime the nonlinear springs are not engaged due to low oscillation amplitudes, therefore, recurring energy exchanges between **E1** and **A1** due to 1:1 resonance dominate the acoustics in a local beat phenomenon. In the intermediate energy (IE) regime, LZT breather redirection occurs

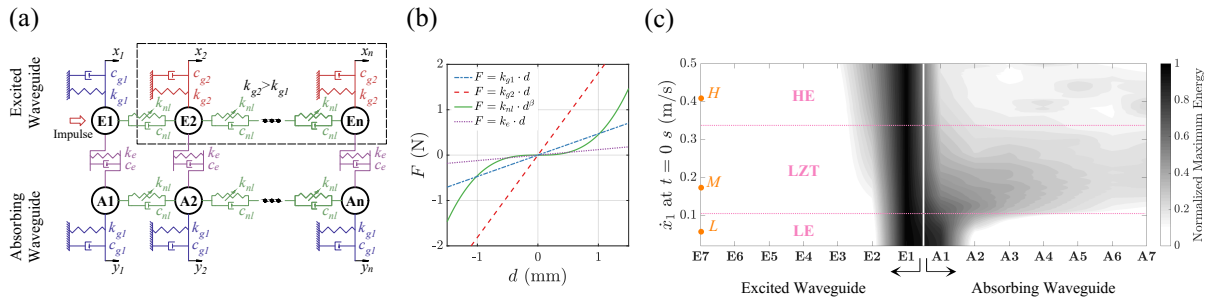


FIG. 1. Theoretical study of macroscale Landau-Zener Tunneling (LZT) in space: (a) Schematic of the reduced-order-model (ROM), (b) force-displacement relations for the stiffnesses used, (c) energy penetration in the 14 unit-cell ROM (see Table I for parameters) for varying initial velocity imposed on unit-cell **E1**; this is represented by contour levels of maximum normalized energy (with respect to input energy) of each unit-cell, with three distinct penetration regimes detected, namely, low energy (LE – point $L$), intermediate energy (IE – point $M$), and high energy (HE – point $H$).

TABLE I. Parameters of the ROM (1).

| $m$ (kg) | $k_{g1}$ (N/m) | $k_{g2}$ (N/m) | $k_e$ (N/m) | $c_{g1}$ (N s/m) | $c_{g2}$ (N s/m) | $k_{nl}$ (N/m$^\beta$) | $\beta$ | $c_{nl}$ (N s/m) |
|---|---|---|---|---|---|---|---|---|
| 0.0245 | 470.25 [30.35] | 1813.2 [39.3] | 121.17 [8.30] | 0.0219 [0.007] | 0.0359 [0.0154] | $2.3 \times 10^8$ | 2.902 | 0.0161 |

from the excited to the absorbing waveguide through 1:1 resonance between **E1** and **A1**, and the model of effective oscillators (3) holds. In the high energy (HE) regime (for $\dot{x}_1(0+) > \sim 0.25$ m/s), intermittent localization in **E1** and wave redirection occur, and much less energy is transmitted to the absorbing waveguide. In this regime, the nonlinearity significantly increases the oscillation frequency of **E1**, preventing sustained 1:1 resonance between **E1** and **A1**. There is a clear boundary between the IE (LZT) and LE regimes, but not between the IE and HE regimes; this is due to viscous damping which perturbs the wave localization in **E1**, yielding complex transition effects at high energies. From FIG. 1(c), LZT irreversible breather redirection from the excited to the absorbing waveguide can be realized only in the IE band, where it is robust to variations in impulse and system parameters. Lastly, we note that the nonlinear asymmetric waveguides of FIG. 1(a) support non-reciprocal acoustics, mainly in the LZT IE regime [16, 22, 23].

## III. EXPERIMENTAL OBSERVATIONS

Guided by the ROM (1), we fabricated an experimental fixture of coupled nonlinear waveguides as in FIG. 2. Each unit-cell is made of a U-shaped aluminum block mass grounded by a pair of thin ($< 130$ μm) copper-beryllium flexure springs with small intrinsic dissipative capacities [24], cf. FIG. 2(b). Within the desired range of oscillation amplitudes, these flexures act as the linear grounding springs of the ROM. The softer ($k_{g1}$) and stiffer ($k_{g2}$) grounding springs of the ROM are realized by modifying the widths of the leaves of the flexures. Within the same waveguide, each unit-cell is coupled to its adjacent ones by two thin 100 μm diameter music wires (cf. FIG. 2) acting as the nonlinear coupling springs of the ROM. Indeed, a straight, initially un-tensioned thin wire, under transverse deformations at its center exhibits essentially nonlinear (non-linearizable) stiffness restoring force approximately of the third order [25], cf. FIG. 1(b); however, acceptable small linear stiffness components are achieved experimentally, by minimizing the unavoidable bending effects and pre-tensions of the wires by means of large length-to-diameter wire ratios and our systematic assembly protocol [21]. Lastly, thick 1 mm diameter spring-steel wires of 10 cm length are clamped between corresponding unit-cells of both waveguides (FIG. 2) to realize the weak linear inter-waveguide coupling stiffnesses $k_e$, cf. FIG. 1.

Accelerometers are used to measure the response of each unit-cell [21]. The measured time series are postprocessed to obtain the energy results of FIG. 3 and 4. Regarding the actuation of the excited waveguide, the unit-cell **E1** is manually forced by a PCB® miniature modal impact hammer. The duration of the impulse is measured as $\sim 2$ μs, i.e., much smaller than the linearized natural period of the unit-cell ($\sim 40$ μs); hence, the experimental impulse meets the computational assumption. Three different impulse intensities are considered, denoted by the three points $L$, $M$, and $H$ in FIG. 1(c). The correspondence with the simulation is based on the ROM (1) with $F(t)$ being the experimentally measured impulse. The data from the impact hammer and the 14 accelerometers is recorded via an m + p VibPlot® dynamic analyzer. Before studying the acoustics, the stiffness and damping parameters of each unit-cell are estimated by system-identification experiments (details are provided in [21]). The estimated parameter variations between unit cells

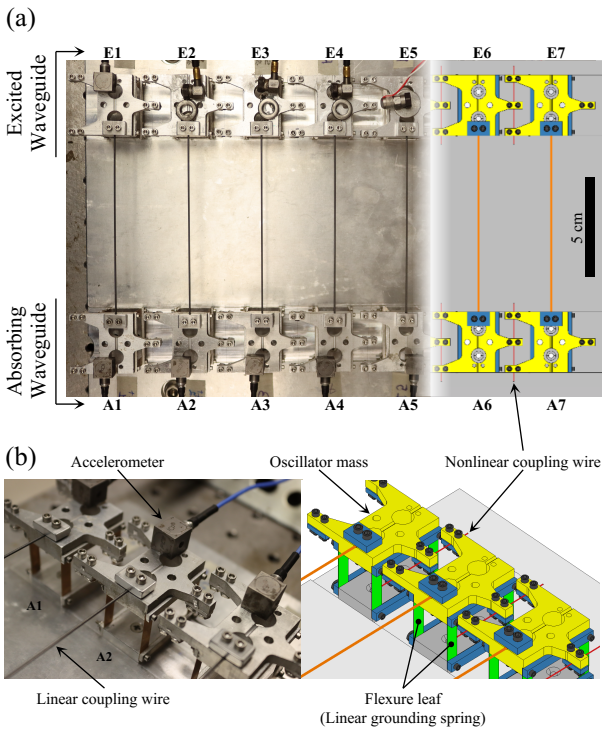


FIG. 2. Experimental fixture of the nonlinear coupled waveguides with 14 unit-cells: (a) Top view with the last 4 unit-cells replaced by schematics for visualization, and (b) isometric (left) and schematic (right) views of unit-cell **A2** connected with **A1** and **A3**; each unit-cell is composed of a U-shaped aluminum block mass (yellow) grounded via a pair of flexure leaves (green), with intra-waveguide nonlinear coupling being realized by thin wires (red), and inter-waveguide linear coupling by thick wires (orange).

due to manufacturing and assembly are small (cf. TABLE I), allowing us to use mean values to simulate the experiments.

FIG. 3 depicts the spatiotemporal evolution of normalized instantaneous energy in the experimental fixture and simulated ROM at the three excitation levels, while FIG. 4 shows the corresponding normalized instantaneous energy envelopes quantifying the energy partition in time between waveguides. The normalizations are with respect to the maximum energy attained [21]. At point $L$ – FIG. 3(a), the impulsive energy gets localized in the leading unit-cells **E1** and **A1**, being continuously and recurrently exchanged between them; this confirms the energy penetration plot in FIG. 1(c). The localization is due to the low impulse, yielding negligibly small nonlinear intra-waveguide coupling. This is noted in FIG. 4(a) with recurrent, complete energy exchanges between **E1** and **A1**. Note the good agreement between experiment and simulation.

Breather redirection due to LZT is confirmed at point $M$ – cf. FIG. 3(b), both experimentally and numerically. The spatiotemporal energy evolution shows irreversible energy transmission from the excited unit-cell **E1** to the absorbing waveguide. It is evident in the experiments that the redirected breather reaches the end unit-cell **A7**, while, the response of the excited waveguide is negligible after the second unit-cell **E2**. Therefore, in the LZT regime the acoustics is reduced, in effect, to a single propagating breather [22, 26] in the absorbing waveguide. In fact, the breather redirection at this intermediate energy level is nearly controlled by the leading unit-cells **E1**, **A1** and **A2** [16]. In this case energy is rapidly and irreversibly transferred from **E1** to **A1**, so the effective oscillator model (3) is valid and provides accurate theoretical prediction of irreversible energy transfer. Moreover, the results in FIG. 4(b) confirm the LZT effect.

At the HE point $H$ – cf. FIG. 3(c), there is a complex state of the acoustics, as within an initial stage of duration $\sim 0.2$ s the input energy is mainly localized in **E1** and **E2**, with a weak propagating breather released to the absorbing waveguide. Following this stage, the energy localization in the excited waveguide nearly ends, and the remaining (diminished) energy is redirected to the absorbing waveguide as a weak propagating breather. In this case viscous damping plays an important role in the acoustics: By dissipating a significant part of the localized energy in the excited waveguide (at a faster scale compared to the previous cases) it enables eventual 1:1 resonance between **E1** and **A1** [16, 27], and, thus, breather redirection. This is confirmed both experimentally and numerically in FIG. 4(c), where up to $\sim 0.2$ s the input energy is mainly localized in the leading unit-cells of the excited waveguide, and then released with time delay to the absorbing waveguide in a similar LZT scenario to point $M$. This, however, occurs only after the localized energy is significantly reduced due to viscous dissipation at a level where nonlinearity becomes less dominant and 1:1 resonance between the unit-cells **E1** and **A1** can be realized; only then, the remaining energy can be finally redirected to the absorbing waveguide. Hence, at high energies there is still irreversible breather redirection from the excited to the absorbing waveguide, albeit time delayed and weaker. Model (3) is not applicable here due to the initial localization in the excited waveguide.

The good agreement at all three energy levels between experiments and simulations in FIG. 3 proves the validity of the ROM (1) with the mean (or typical) parameter values of TABLE I. There is some deviation between experiments and simulations in the plots of FIG. 4, caused by postprocessing errors in estimating the initial velocity of the unit-cell **E1** [21]; these errors originate from the high "drifts" in the accelerometer measurements due to sudden velocity jumps immediately following the applied impulses by the impact hammer. The drift errors account for the sudden initial energy decreases in the experimental plots of FIG. 4 – within milliseconds of the application of the impulse to **E1**, and the uniformly lower experimental energies compared to the simulated ones. Apart from this discrepancy, however, the experimental results confirm the three theoretically predicted response regimes,

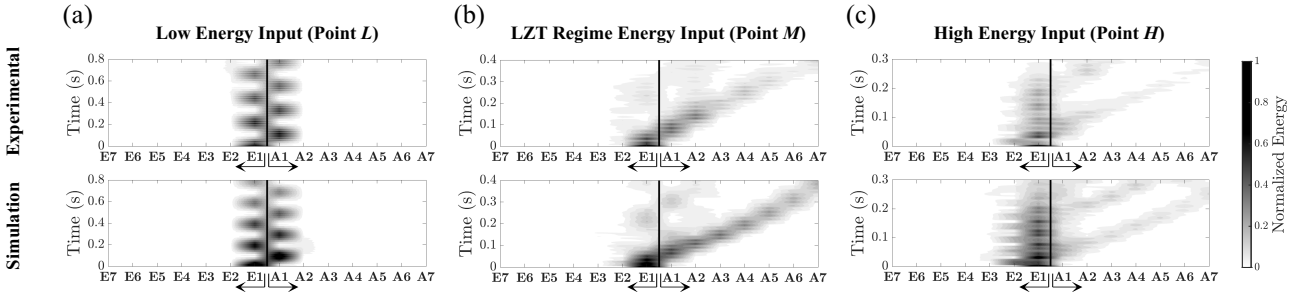


FIG. 3. Spatiotemporal evolution of normalized energy in the experimentally tested fixture (top) and simulated ROM (bottom) when subjected to (a) low, (b) intermediate, and (c) high energy input – cf. FIG. 1(c).

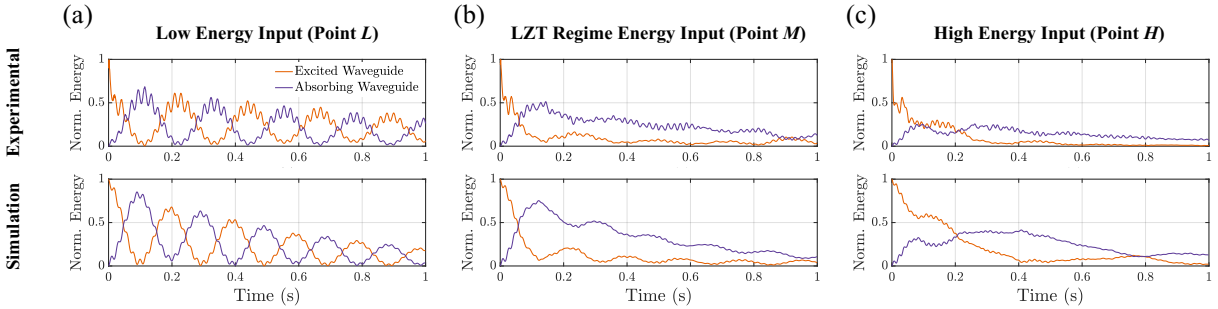


FIG. 4. Experimental (top) and simulated (bottom) envelopes of normalized energies of the excited (orange) and absorbing (purple) waveguides as functions of time, (a-c) as in FIG. 3.

and more importantly, the LZT-based breather redirection in the IE regime. Lastly, the passive self-tunability of the acoustics and the irreversible breather redirection due to the strong stiffness nonlinearity are experimentally proved.

## IV. CONCLUSIONS

Experimental validation of a macroscale analog of classical quantum Landau-Zener Tunneling (LZT) was presented and applied for irreversible wave redirection in weakly coupled and disordered nonlinear waveguides under impulse excitation. The strong stiffness nonlinearity yields passive self-tunability of the acoustics to energy, switching between localization and wave redirection depending on the impulse intensity. Such inherent and passive self-tunable wave tailoring is not possible in linear time-invariant settings. The results highlight the efficacy of LZT-based passive wave redirection in a broad class of acoustical systems combining nonlinearity, disorder and weak coupling, with potential applications in shock mitigation, solid state, ultrasonics, metamaterials, acoustic surface wave devices, structural logic and optics. Finally, we note that the realization of passive energy redirection inflicts break of acoustic reciprocity in the considered lattices, which can have additional applications in nonlinear acoustics.

## ACKNOWLEDGMENTS

This work was supported in part by NSF Emerging Frontiers Research Initiative (EFRI) Grant 1741565.

[1] L. D. Landau, A theory of energy transfer ii, Phys. Z. Sowjetunion **2**, 19 (1932).
[2] C. Zener, Non-adiabatic crossing of energy levels, Proceedings of the Royal Society of London. Series A, Containing Papers of a Mathematical and Physical Character **137**, 696 (1932).
[3] H. Schneider, H. Grahn, K. v. Klitzing, and K. Ploog, Resonance-induced delocalization of electrons in gaas-alas superlattices, Physical review letters **65**, 2720 (1990).
[4] B. Rosam, K. Leo, M. Glück, F. Keck, H. Korsch, F. Zimmer, and K. Köhler, Lifetime of wannier-stark states in semiconductor superlattices under strong zener tunneling

to above-barrier bands, Physical Review B **68**, 125301 (2003).
[5] C. Bharucha, K. Madison, P. Morrow, S. Wilkinson, B. Sundaram, and M. Raizen, Observation of atomic tunneling from an accelerating optical potential, Physical Review A **55**, R857 (1997).
[6] B. P. Anderson and M. A. Kasevich, Macroscopic quantum interference from atomic tunnel arrays, Science **282**, 1686 (1998).
[7] M. Cristiani, O. Morsch, J. Müller, D. Ciampini, and E. Arimondo, Experimental properties of bose-einstein condensates in one-dimensional optical lattices: Bloch oscillations, landau-zener tunneling, and mean-field effects, Physical Review A **65**, 063612 (2002).
[8] C. Sias, A. Zenesini, H. Lignier, S. Wimberger, D. Ciampini, O. Morsch, and E. Arimondo, Resonantly enhanced tunneling of bose-einstein condensates in periodic potentials, Physical review letters **98**, 120403 (2007).
[9] H. Sanchis-Alepuz, Y. A. Kosevich, and J. Sánchez-Dehesa, Acoustic analogue of electronic bloch oscillations and resonant zener tunneling in ultrasonic superlattices, Physical Review Letters **98**, 134301 (2007).
[10] J. Sánchez-Dehesa, H. Sanchis-Alepuz, Y. A. Kosevich, and D. Torrent, Acoustic analog of electronic bloch oscillations and zener tunneling, The Journal of the Acoustical Society of America **120**, 3283 (2006).
[11] Z. He, S. Peng, F. Cai, M. Ke, and Z. Liu, Acoustic bloch oscillations in a two-dimensional phononic crystal, Physical Review E **76**, 056605 (2007).
[12] M. de Lima Jr, Y. A. Kosevich, P. Santos, and A. Cantarero, Surface acoustic bloch oscillations, the wannier-stark ladder, and landau-zener tunneling in a solid, Physical review letters **104**, 165502 (2010).
[13] Y. A. Kosevich, L. I. Manevitch, and E. Manevitch, Vibrational analogue of nonadiabatic landau–zener tunneling and a possibility for the creation of a new type of energy traps, Physics-Uspekhi **53**, 1281 (2010).
[14] L. I. Manevitch, Y. A. Kosevich, M. Mane, G. Sigalov, L. A. Bergman, and A. F. Vakakis, Towards a new type of energy trap: Classical analog of quantum landau-zener tunneling, International Journal of Non-Linear Mechanics **46**, 247 (2011).
[15] M. Hasan, Y. Starosvetsky, A. Vakakis, and L. Manevitch, Nonlinear targeted energy transfer and macroscopic analog of the quantum landau–zener effect in coupled granular chains, Physica D: Nonlinear Phenomena **252**, 46 (2013).
[16] C. Wang, S. Tawfick, and A. F. Vakakis, Irreversible energy transfer, localization and non-reciprocity in weakly coupled, nonlinear lattices with asymmetry, Physica D: Nonlinear Phenomena **402**, 132229 (2020).
[17] Y. A. Kosevich, L. Manevitch, and A. Savin, Energy transfer in coupled nonlinear phononic waveguides: transition from wandering breather to nonlinear self-trapping, in *Journal of Physics: Conference Series*, Vol. 92 (Institute of Physics and IOP Publishing Limited, 2007) pp. 012093–012093.
[18] Y. A. Kosevich, L. I. Manevitch, and A. V. Savin, Wandering breathers and self-trapping in weakly coupled nonlinear chains: classical counterpart of macroscopic tunneling quantum dynamics, Physical Review E **77**, 046603 (2008).
[19] Y. A. Kosevich, L. I. Manevitch, and A. V. Savin, Energy transfer in weakly coupled nonlinear oscillator chains: Transition from a wandering breather to nonlinear self-trapping, Journal of sound and vibration **322**, 524 (2009).
[20] Y. Starosvetsky, M. A. Hasan, A. F. Vakakis, and L. I. Manevitch, Strongly nonlinear beat phenomena and energy exchanges in weakly coupled granular chains on elastic foundations, SIAM Journal on Applied Mathematics **72**, 337 (2012).
[21] See supplemental material at [link to be inserted by publisher] for tables of identified parameters of the fixture, and detailed explanations related to the assembly protocols, the system identification experiments, the post-processing of measurements, and videos of wave localization and lzt wave redirection., .
[22] A. Mojahed, O. V. Gendelman, and A. F. Vakakis, Breather arrest, localization, and acoustic non-reciprocity in dissipative nonlinear lattices, The Journal of the Acoustical Society of America **146**, 826 (2019).
[23] A. Mojahed, J. Bunyan, S. Tawfick, and A. F. Vakakis, Tunable acoustic nonreciprocity in strongly nonlinear waveguides with asymmetry, Physical Review Applied **12**, 034033 (2019).
[24] M. Ashby and A. Greer, Metallic glasses as structural materials, Scripta Materialia **54**, 321 (2006).
[25] D. M. McFarland, L. A. Bergman, and A. F. Vakakis, Experimental study of non-linear energy pumping occurring at a single fast frequency, International Journal of Non-Linear Mechanics **40**, 891 (2005).
[26] A. Mojahed and A. F. Vakakis, Certain aspects of the acoustics of a strongly nonlinear discrete lattice, Nonlinear Dynamics **99**, 643 (2020).
[27] L. Manevitch, New approach to beating phenomenon in coupled nonlinear oscillatory chains, Archive of Applied Mechanics **77**, 301 (2007).
[28] H. E. Rauch, F. Tung, and C. T. Striebel, Maximum likelihood estimates of linear dynamic systems, AIAA journal **3**, 1445 (1965).
[29] K. Murphy, Kalman filter toolbox for matlab, Computer Science and Artificial Intelligence Lab., MIT (1998).
[30] S. B. Kim, B. Spencer Jr, and C.-B. Yun, Frequency domain identification of multi-input, multi-output systems considering physical relationships between measured variables, Journal of Engineering Mechanics **131**, 461 (2005).
[31] D. J. Ewins, *Modal Testing: Theory, Practise and Application*, 2nd ed. (Wiley, New York, 2009).
[32] D. M. McFarland, L. A. Bergman, and A. F. Vakakis, Experimental study of non-linear energy pumping occurring at a single fast frequency, International Journal of Non-Linear Mechanics **40**, 891 (2005).
[33] A. F. Vakakis, O. V. Gendelman, L. A. Bergman, D. M. McFarland, G. Kerschen, and Y. S. Lee, *Nonlinear targeted energy transfer in mechanical and structural systems*, Vol. 156 (Springer Science & Business Media, 2008).